Liquid Crystals
Publication details, including instructions for authors and subscription information:
http://www.informaworld.com/smpp/title~content=t713926090

Thermophysical study of lead(II) *n*-alkanoates by DSC, optical microscopy, FTIR and Raman spectroscopy

A. Sanchez Arenas[a]; M. V. Garcia[a]; M. I. Redondo[a]; J. A. R. Cheda[a]; M. V. Roux[b]; C. Turrion[b]
[a] Departamento de Química Física, Facultad Ciencias Químicas Universidad Complutense, Madrid, Spain [b] Instituto de Química Física Rocasolano, (C.S.I.C.), Madrid, Spain

To cite this Article Arenas, A. Sanchez , Garcia, M. V. , Redondo, M. I. , Cheda, J. A. R. , Roux, M. V. and Turrion, C.(1995) 'Thermophysical study of lead(II) *n*-alkanoates by DSC, optical microscopy, FTIR and Raman spectroscopy', Liquid Crystals, 18: 3, 431 — 441
To link to this Article: DOI: 10.1080/02678299508036642
URL: http://dx.doi.org/10.1080/02678299508036642

LIQUID CRYSTALS, 1995, VOL. 18, NO. 3, 431–441

Thermophysical study of lead(II) *n*-alkanoates by DSC, optical microscopy, FTIR and Raman spectroscopy

by A. SANCHEZ ARENAS, M. V. GARCIA, M. I. REDONDO
and J. A. R. CHEDA*

Departamento de Química Física,
Facultad Ciencias Químicas Universidad Complutense, 28040 Madrid, Spain

M. V. ROUX and C. TURRION

Instituto de Química Física Rocasolano, (C.S.I.C.), Serrano, 119,
28006 Madrid, Spain

(*Received 14 February 1994; in final form 2 June 1994; accepted 14 June 1994*)

Thirteen members of the lead(II) *n*-alkanoate series (from the *n*-hexanoate to the *n*-octadecanoate) have been synthesized, purified, and studied by differential scanning calorimetry, polarizing light microscopy, and FTIR and Raman spectroscopy. A solid–solid transition was found for all members of the series. A mesomorphic state, implying a fusion and a clearing point, was identified as smectic C, and was present only in the lower members of the series below the *n*-tridecanoate. The higher members form the isotropic liquid through a regular fusion. Temperatures and enthalpies for the phase transitions have been measured and the corresponding entropy changes calculated. Heat capacity measurements between 280 K and 400 K were also carried out. A study of these magnitudes versus number of carbons was made. The solid phase previous to the liquid crystal in the lower members and to the isotropic liquid in the higher members could be identified as a 'condis' crystal (conformationally disordered phase) by an FTIR versus temperature study.

1. Introduction

The lead(II) *n*-alkanoates belong to the big family of so called organic salts and are interesting because of both their polymorphism, thermotropic and lyotropic mesomorphism (plastic or ionic liquid crystals), and the ease of 'moving' a particular physical property to a desired condition by changing the size or shape of the organic ion and/or the inorganic counter ion. Many studies have been published recently such as the Franzosini and Sanesi revision [1] or the Mirnaya *et al.* [2], review, where an increasing interest due to industrial applications of the ionic liquid crystals is claimed. The step-wise melting process of organic salts from the very well-ordered structure at low temperatures (CH_2 groups in an all-*trans*-conformation) to the isotropic liquid is an important point of interest of these families of compounds. In this sense, the thallium(I) *n*-alkanoates series has proved to be one of the most representative for understanding this melting process [3]. Within the *n*-alkanoate series, the behaviour is completely different when changing the valence of the cation. This is one of the reasons why we have chosen the lead(II) *n*-alkanoates. Another reason is that, even although several studies have been made of this series, many discrepancies appear among the different authors. Adeosun and Sime [4] were the first to study some even members of the lead(II) series by DTA and polarizing light microscopy. Later, they studied some odd members too, obtaining similar results [5]. They proposed two liquid crystal structures for the lower members of the series below the *n*-dodecanoate, and only one mesophase above the *n*-tetradecanoate. Ellis also studied some even lead(II) *n*-alkanoates [6, 7] by DSC, X-ray diffraction, and polarizing light microscopy, and was in disagreement with other authors with regard to the existence of two mesophases. Ellis claimed the existence of only one mesophase for the lower members and two solid phases for all of them. His conclusion was based on the relatively large enthalpy values measured for the lower temperature phase transitions. Burrows *et al.* [8–15], carried out a study on some members of the series using different techniques such as DSC, polarizing light microscopy. X-ray diffraction, multi-nuclear NMR, Raman and IR spectroscopy, densities, etc. An ordered mesophase followed by a more disordered phase were proposed for the lower members of the series. Summarizing, there are discrepancies not only

* Author for correspondence.

0267–8292/95 $10·00

concerning the assignment of the intermediate phase as solid or mesophase, but also about the description of its structure. Therefore, whilst Ellis and De Vries [7] say that the chains are tilted with respect to the ionic layers, Burrows *et al.* [10], disagree. Moreover, there are also discrepancies in the experimental data on the Bragg spacings for the crystals for $n = 14$, 16, 18 reported by the two groups of authors.

In this study, special attention has been paid to the purity of the samples studied during their preparation. A thorough thermal study of the transitions for recrystallized and premelted samples was made by DSC, and measurements of the molar heat capacity complete this thermal information. Polarizing light microscopy was used in the identification of the mesophase. To understand the step-wise melting process taking place in this series of compounds, on going from the all-trans completely ordered solid to the isotropic liquid, FTIR experiments as a function of temperature were also carried out. Raman spectroscopy was used to help in understanding differences in the crystalline structure in the solid state.

2. Experimental

2.1. *Sample preparation*

The lead(II) *n*-alkanoates studied (named hereafter Pb(C*n*)$_2$, where *n* is the number of carbons in the organic anion, including the carboxylic carbon atom) were prepared following a method described elsewhere [16]. This consists in the metathesis of the potassium ion from the corresponding *n*-alkanoate in absolute ethanol (Merck, p.a.) solution by the lead(II) ion, added as the nitrate (Merck. p.a.) dissolved in a small amount of water. The potassium *n*-alkanoate had been prepared previously by direct interaction of potassium hydroxide (Fluka, puriss., p.a.) with the *n*-alkanoic acid (HC*n* puriss. from Fluka, except for HC8, HC9, HC15 and HC18, which were from Merck) dissolved in absolute ethanol (Merck), with gentle heating at about 70°C.

Several recrystallizations from benzene were necessary to achieve a high purity. In table 1, the results for the mol per cent purity obtained by the DSC fractional fusion technique [17] are included. Particular details for some compounds are given as footnotes.

2.2. *Differential scanning calorimetry*

A Perkin–Elmer DSC-2C, connected to a Model 3600 Data Station, with TADS system, was used between 290 K and 400 K, the temperature range of interest in this study. The temperature scale was calibrated by measuring the melting points of recommended high purity standards: *n*-pentadecane, *n*-octadecane, gallium, indium, tin, and *n*-octadecanoic and benzoic acids. The power scale was calibrated using high purity indium (> 99·999 mol per cent) as the standard material.

Thermograms of samples in sealed aluminium pans were recorded over the entire temperature range in a nitrogen atmosphere at scanning rates of 10, 5, and 2·5 K min^{-1}, and a range of 2 mcal s^{-1}. Four to six samples of each compound weighing 5 to 15 mg were used for the enthalpy determinations. The values given are the mean values of the results. The estimated errors were ± 0·5 K and about 2 per cent for temperatures and enthalpies, respectively. Heat capacities were determined by the heat capacity program of TADS. Synthetic sapphire was used as standard material for checking the program. The complete temperature range for the determination of the heat capacities was divided into approximately 30 K intervals, overlapping five degrees one with another. The heat capacity values were the average of four experiments for each compound. The estimated error in the heat capacity was about 2 per cent.

2.3. *Optical microscopy*

A Jena–Zeiss, Jenalab-pol model, polarizing light microscope was used in the identification of the different solid and mesomorphic phases of the lead(II) *n*-alkanoates. To control the temperature during the microscopic observations, Mettler FP-80 equipment, consisting of a DTA stage with two glass windows, which allowed the corresponding thermograms to be obtained, was used simultaneously. The samples were examined inside the regular Pyrex glass capsules with a glass cover, previously cleaned and rubbed in one direction with acetone, in order to avoid formation of the homeotropic texture of the mesophase. In this way, the non-homeotropic texture was formed on cooling the samples from the isotropic liquid. Pictures were recorded on regular film.

2.4. *Vibrational spectroscopy*

Infrared spectra of samples prepared as KBr pellets were recorded using an FTIR Nicolet 60SX instrument working at a resolution of 2 cm^{-1}. Thirty two scans were averaged to give the final spectra. A VTL-2 variable temperature cell was used to obtain spectra every 5 degrees from room temperature to about 400 K. Raman spectra were excited using the 514·5 nm line of an Ar^+ laser and obtained using a Dilor XY instrument using a spectral slit width of about 5 cm^{-1}.

3. Experimental results

3.1. *Differential scanning calorimetry*

In figure 1, thermograms for the specified compounds are shown. From these, particular aspects of behaviour may be inferred. For Pb(C6)$_2$, only two transitions are recorded on the first heating for the fresh sample. On

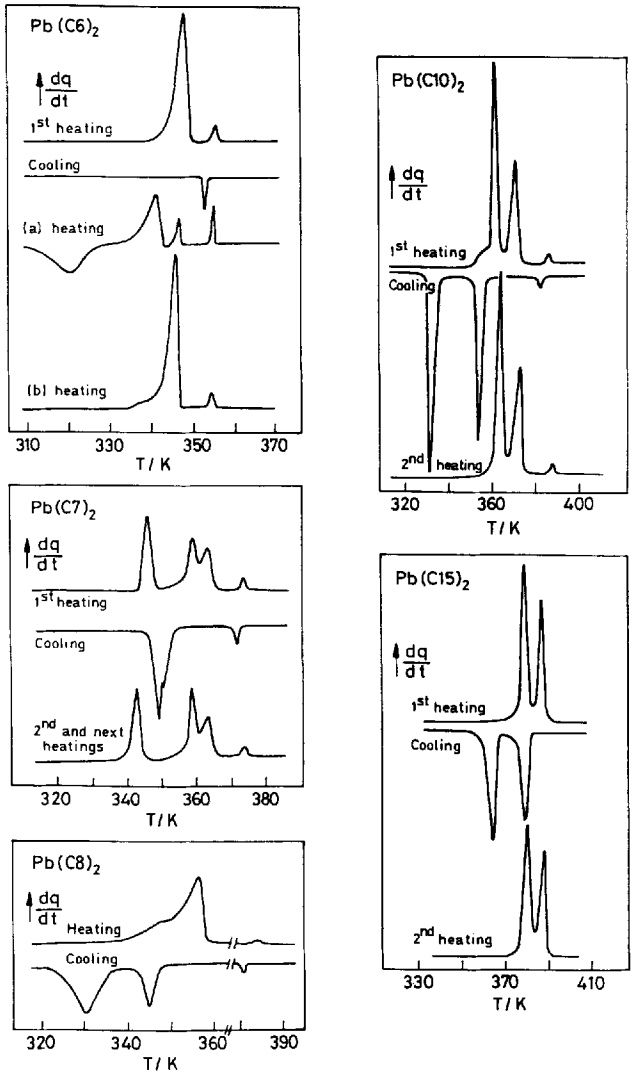

Figure 1. Thermal behaviour of $Pb(Cn)_2$; $n = 6, 7, 8, 10, 15$. Details for $Pb(C6)_2$—see text. Heating rate = 5 K min^{-1}, except for $Pb(C8)_2$ which was 1 K min^{-1}. Range 5 mcal s^{-1}.

cooling from the isotropic liquid, a large supercooling effect is observed in the transition taking place at about 340 K. Two different behaviours are observed on the second and subsequent heatings, depending on the delay time in registering the thermogram (see figure 1, $Pb(C6)_2$ (*a*) and (*b*); (*a*) corresponds to the thermogram obtained immediately after cooling; (*b*) is obtained when the delay time is 75 min at 300 K); a small shoulder is observed before the first transition. No differences are observed in the thermograms obtained for $Pb(C7)_2$ and $Pb(C8)_2$ between first and subsequent heatings. $Pb(C7)_2$ presents one transition more than the other short members of the series. For $Pb(C10)_2$, a shoulder is observed previous to the first transition on the first heating; this disappears on the second heating. This behaviour is common to the members with $n = 9$–12. The thermograms for $Pb(C15)_2$ are given as an example of what is observed for members with $n = 13$–18. In these samples, the thermal behaviour is the same as on the first heating. The different behaviours of the crystallized and melted samples can be attributed to the occurrence of polytipism [18] in some members of this series ($n = 6, 9, 10, 11, 12$). After the second scan, the thermal behaviour of all the samples is reversible. All the compounds were explored by DSC from 80 K up to 290 K, and no phase transitions were observed.

In table 1, the experimental values for the temperatures (read from thermograms corresponding to previously melted samples), enthalpies, and entropies are given. In figure 2, the temperatures of transitions are represented on a linear scale. The assignments for the phases proposed by different authors are given in the same figure. The experimental results for the molar heat capacities are shown in table 2.

3.2. *Optical microscopy*

Solid–solid, fusion, and clearing transitions were observed for the members with $6 \leqslant n \leqslant 12$, and only one solid–solid transition and regular fusion for the members with $n \geqslant 13$. The designation of the different solid, mesomorphic and isotropic liquid states is based on the polarizing light microscopic observations. With this technique, the mesophase was identified as smectic C (sanded texture) [19], in agreement with Ellis and De Vries [7]. Amorin da Costa *et al.* [8], identified this phase as smectic A and Adeosun and Sime [4] as cubic isomorphic. In figure 3, photomicrographs of $Pb(C7)_2$ are shown at the specified temperatures, as an example of the general behaviour of all the compounds presenting mesophases. As usual, the liquid crystal structure appears only on cooling from the isotropic liquid. The white needles of the intermediate phase, solid **I** in our nomenclature, are seen for all members of the series. The nature of this phase has been a point of discussion; whilst Ellis considered this phase as a solid [6, 7], Adeosun *et al.* [4, 5], Amorin da Costa *et al.* [8], and Burrows *et al.* [9–11], claimed it was a highly ordered smectic mesophase. On heating this solid **I** phase, needles remain and only a change to a blue colour is observed at the transition to the liquid crystal.

3.3. *Vibrational spectroscopy*

Typical IR and Raman spectra of the compounds are shown in figure 4. Table 3 summarizes the most characteristic vibrational wavenumbers found for these samples. Vibrational spectra of all the compounds studied here are very similar. In all the spectra obtained at room temperature, the band corresponding to vibrations of the carboxylate group (symmetric and asymmetric stretching and bending) was split into two components which seems

Table 1. Purities and thermal functions of the phase transitions of lead(II) *n*-alkanoates on samples previously melted.

Carbon chain length	Purity	Transition	T/K	ΔH/kJ mol^{-1}	ΔS/J K^{-1} mol^{-1}
6†	98·9‡	SII–SI	333·6	1·86	5·58
		SI–LC	341·2	18·63	54·60
		LC–IL	352·2	1·20	3·41
7	§	SII–SI	343·2	12·55	36·57
		SI–LC	356·7	6·40	17·94
		(Two steps)	359·8	5·90	16·40
		LC–IL	373·2	1·09	2·92
8	§	SII–SI	346·4‖	24·03b	69·38¶
		SI–LC	350·6‖	10·46b	29·83¶
		LC–IL	384·4	1·22	3·17
9	99·7	SII–SI	350·6	30·27	86·32
		SI–LC	369·2	16·22	43·94
		LC–IL	386·2	1·07	2·77
10	99·9	SII–SI	359·4	34·71	96·58
		SI–LC	370·4	19·96	53·89
		LC–IL	387·5	1·01	2·61
11	98·9	SII–SI	361·1	40·80	113·00
		SI–LC	377·4	22·42	59·41
		LC–IL	386·0	0·85	2·20
12	99·7	SII–SI	367·3	49·25	134·07
		SI–LC	377·5	28·80	76·29
		LC–IL	384·4	0·91	2·37
13	99·5	SII–SI	372·4	51·69	138·82
		SI–IL	382·5	33·20	87·05
14	99·7	SII–SI	374·1	55·66	148·80
		SI–IL	382·5	38·13	99·69
15	99·6	SII–SI	376·8	60·08	159·44
		SI–IL	385·4	42·95	111·43
16	99·7	SII–SI	377·8	67·36	178·30
		SI–IL	385·0	50·64	131·54
17	99·8	SII–SI	382·3	69·33	181·33
		SI–IL	387·6	54·37	140·27
18	99·5	SII–SI	383·8	76·11	198·32
		SI–IL	387·9	57·84	149·11

†After waiting for thermal equilibrium.

‡Measured for the first fusion on the recrystallized compound.

§Despite three (or more) recrystallizations during sample preparation of these compounds, the solid–solid and the fusion transitions are so close to each other that separation of both—even at very low heating rates—is not possible; consequently purity determination was impossible.

‖Total energy measured on heating proportionately divided according to the areas of the two peaks observed completely separated on cooling.

¶'Onset' temperature of fusion read after deconvolution of the peak obtained on heating.

SII = solid **II**; SI = solid **I**; LC = liquid crystal; IL = isotropic liquid.

to confirm the asymmetrical environment of the carboxylate group determined by Feio *et al.* [13], for solid lead(II) decanoate and octadecanoate from high-resolution ^{13}C NMR spectra. The most notable difference between the spectra of different compounds is the number of CH_2 wagging progression bands observed in the infrared as a set of regularly spaced bands (see figure 5). These bands are characteristic of chains in the all-trans-conformation and their number depends on the number of CH_2 units in the alkyl chain [20]. Infrared spectra taken at different temperatures show that the intensity of these bands decreases on increasing the temperature and finally the regular pattern is lost (see figure 5) at a temperature close to that corresponding to the solid–solid transition as

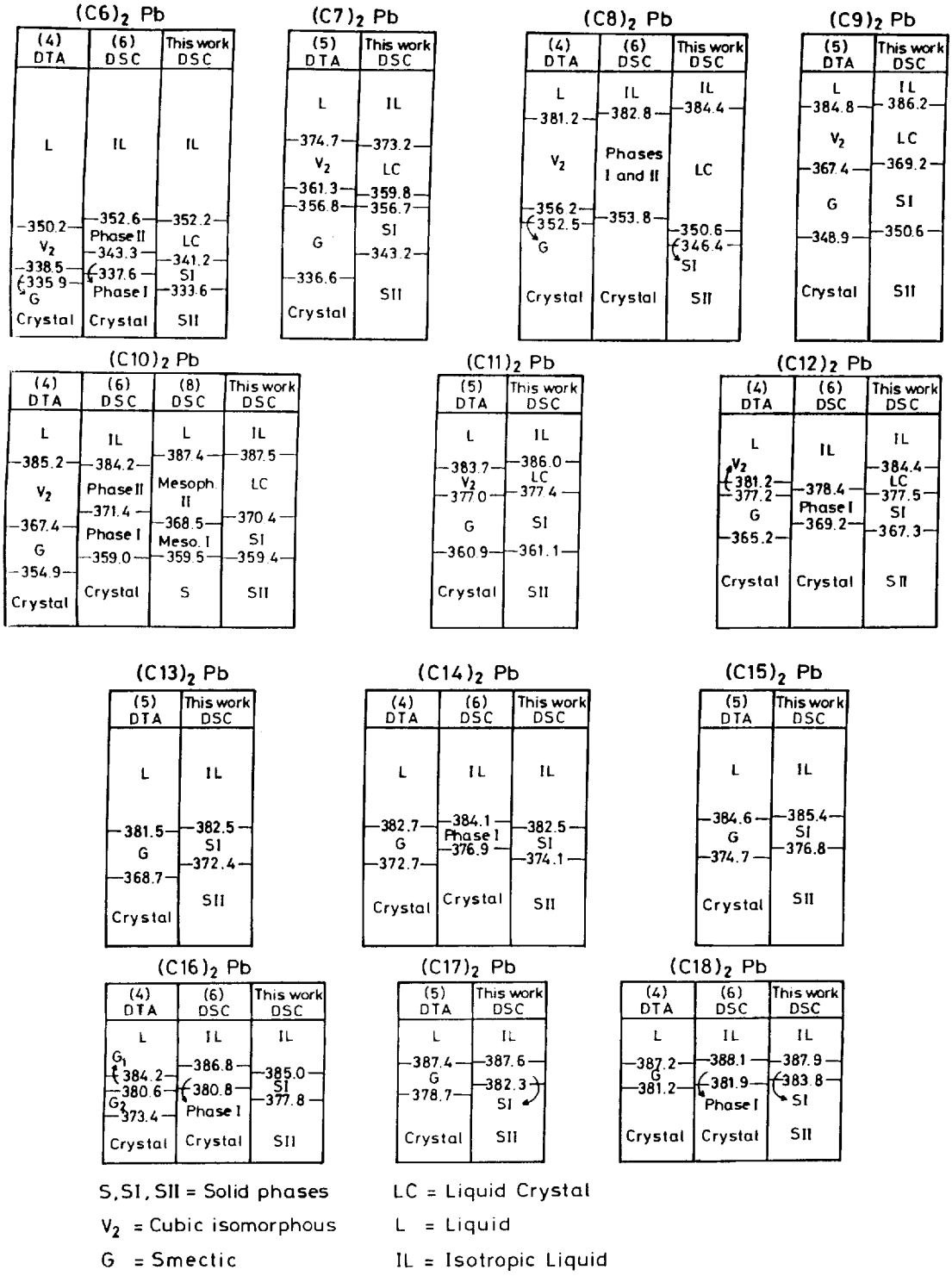

Figure 2. Schematic representation of the temperatures of the transitions and the phase assignments given by different authors to the phases of the Pb(C*n*)$_2$ series.

Table 2. Molar heat capacities of lead(II) *n*-alkanoates.

	C_p/J K^{-1} mol^{-1}												
T/K	$Pb(C6)_2$	$Pb(C7)_2$	$Pb(C8)_2$	$Pb(C9)_2$	$Pb(C10)_2$	$Pb(C11)_2$	$Pb(C12)_2$	$Pb(C13)_2$	$Pb(C14)_2$	$Pb(C15)_2$	$Pb(C16)_3$	$Pb(C17)_2$	$Pb(C18)_2$
281	—	—	—	—	—	—	—	—	674·88	—	—	—	—
282	—		438·67	—	—	—	—	—	677·04	—	—	—	—
283	363·76	399·17	441·83	—	504·77	540·02	581·76	624·91	688·85	—	—	—	—
285	371·24	407·24	449·72	—	510·67	551·49	603·96	637·63	693·34	—	—	—	—
290	383·29	418·55	462·53	485·64	529·63	567·54	611·02	645·36	700·32	735·08	780·64	809·16	856·80
295	394·85	430·27	472·42	497·87	536·86	579·51	621·42	647·69	719·78	758·44	800·93	829·53	882·91
300	404·41	440·91	482·15	507·26	544·34	592·48	628·98	658·83	727·09	777·23	814·31	846·57	903·11
305	414·80	454·63	499·11	515·33	551·00	595·81	643·53	682·44	741·98	792·20	836·59	864·20	912·09
310	420·79	464·52	515·41	524·31	566·88	613·94	653·43	685·60	755·11	807·00	857·05	882·74	930·55
315	426·78	480·07	537·44	533·45	582·26	628·65	670·06	695·42	772·91	817·06	877·17	916·58	953·58
320	437·25	494·87	555·65	543·10	592·15	639·22	681·78	714·79	789·28	822·79	905·19	929·38	971·04
325	446·32	514·50	576·70	552·24	610·11	657·42	700·74	729·42	802·84	843·91	916·66	944·68	987·67
330	460·62	538·02	609·44	560·97	622·08	676·96	716·96	739·73	822·79	858·05	927·89	963·39	1005·04
335	493·29	621·34	808·32	575·60	634·72	702·90	724·18	758·94	835·35	881·74	947·51	983·43	1022·59
337	514·58	—	—	580·01	642·45	715·70	734·33	763·10	849·23	884·65	957·15	995·32	1033·56
340	—	—	—	590·90	652·10	724·35	740·98	764·09	861·95	898·20	968·30	1011·53	1050·94
344	—	—	—	611·61	665·82	748·13	753·78	783·30	885·23	916·41	992·07	1033·31	1070·40
345	—	—	—	—	667·81	751·04	759·44	789·78	884·82	920·74	997·73	1031·90	1074·97
349	—	—	—	—	682·28	795·60	772·08	805·83	905·77	942·10	1014·61	1052·10	1094·34
350	—	—	—	—	684·44	810·49	770·41	803·25	907·77	—	1013·69	1056·01	1094·01
355	—	—	—	—	708·80	896·87	783·38	828·70	924·48	—	1040·30	1081·70	1120·70
360	—	—	—	—	—	—	805·08	833·27	945·68	—	1064·74	1098·66	1139·74
365	—	—	—	—	—	—	—	846·57	974·61	—	1104·65	1126·77	1171·25
366	—	—	727·43	—	—	—	—	855·05	989·25	—	1116·62	1132·92	1179·73
369	—	—	733·41	—	—	—	—	883·32	1008·45	—	1143·64	1153·79	1204·92
370	—	—	734·49	—	—	—	—	—	—	—	1162·19	1158·61	1210·83
375	—	—	738·48	—	—	—	—	—	—	—	—	1215·15	1267·53
377	—	—	742·48	—	—	—	—	—	—	—	—	1270·11	1306·86
378	—	—	739·15	—	—	—	—	—	—	—	—	—	1318·75
380	—	—	742·81	—	—	—	—	—	—	—	—	—	—
385	—	—	747·46	—	—	—	—	—	—	—	—	—	—
388	—	—	985·09	—	—	—	—	—	—	—	—	—	—

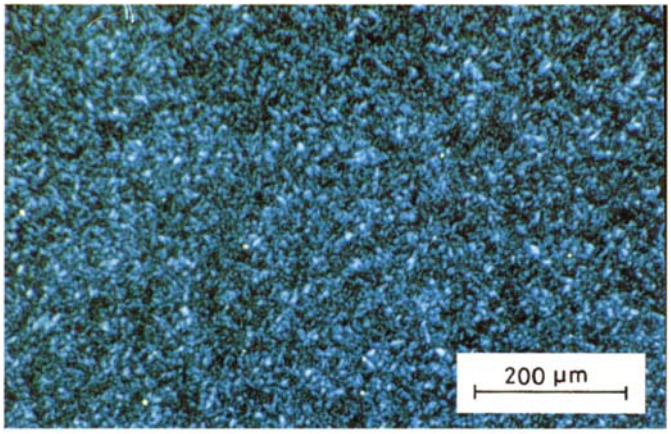

(*a*)

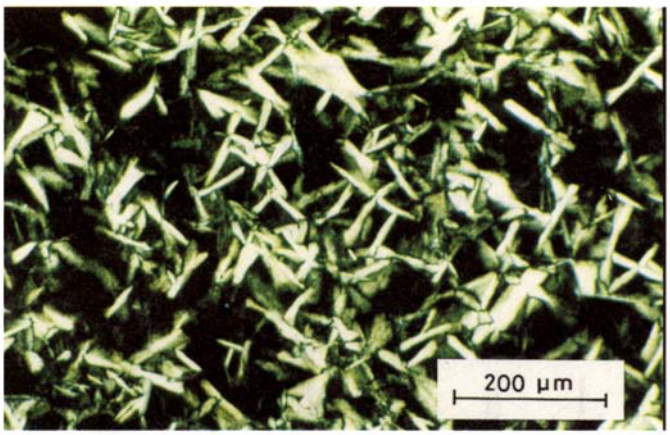

(*b*)

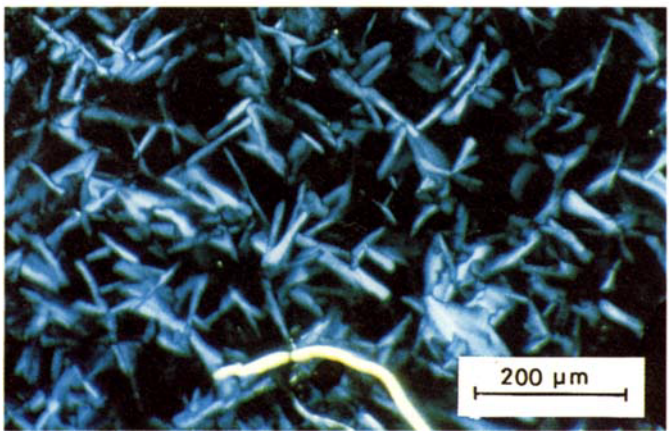

(*c*)

Figure 3. Textures observed by polarizing light microscopy with crossed polars for $Pb(C7)_2$. (*a*) Liquid crystal (smectic C, broken fan texture, (sanded)), at 370 K, on cooling from the isotropic liquid. (*b*) Solid **I**, at 328·8 K. (*c*) Liquid crystal phase on heating at 370 K.

measured by DSC. In addition, a band around 1306 cm^{-1} characteristic of GTG′ and GTG ('kink') structures is observed at this same temperature. The intensity of this

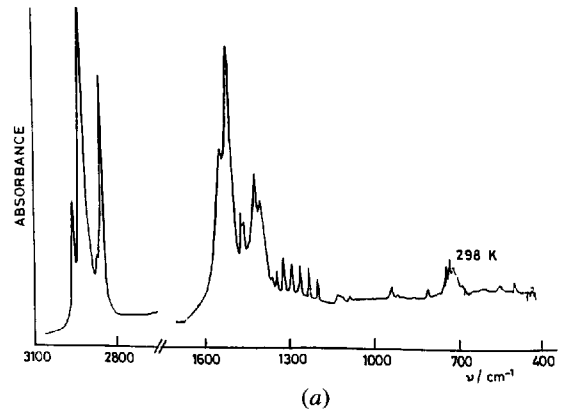

(*a*)

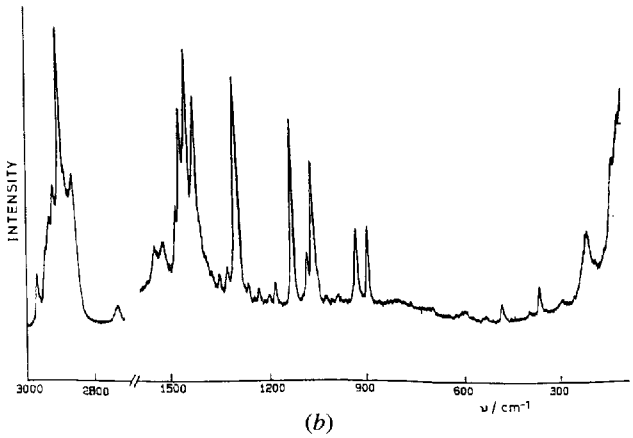

(*b*)

Figure 4. Infrared (*a*) and Raman (*b*) spectra of $Pb(C11)_2$ (recrystallized sample).

band increases slowly from this temperature up to that of the isotropic liquid. There are some bands clearly dependent on the thermal history of the samples, although this effect is most noticeable in the Raman spectra where some bands are specially sensitive to changes in the crystalline structure of the compounds. For instance, as can be seen in figure 6, Raman spectra of crystallized $Pb(Cn)_2$ from $n = 9$–12 show the crystal-field splitting components of the CH_2 scissoring mode at about 1417 and 1440 cm^{-1}, while, in the premelted samples, these bands appear at 1422 and 1440 cm^{-1} and a new strong band is observed at 1407 cm^{-1}. Infrared and Raman spectra of both crystallized and premelted samples change at the same fixed temperature.

4. Discussion

4.1. *Thermal behaviour*

Comparison of the data in table 1 with results from [4–6] and [8], show that our melting and clearing temperatures are higher than those in the literature in almost all cases, and that there are discrepancies in the results reported by

Table 3. Characteristic vibrational wavenumber (ν/cm^{-1}) observed for lead(II) alkanoates.

Raman			
Infrared	Crystallized	Premelted	Assignment
2955	2963	2963	$\nu_a(CH_3)$
2919	2933	2933	$\nu_a(CH_2)_\alpha$
	2885	2890	$\nu_a(CH_2)$ Fermi resonance†
2870	2874	2874	$\nu_a(CH_2)$
2850	2850	2850	$\nu_s(CH_2)$
1542 } 1512 }	1536 } 1513 }	1517	$\nu_a(COO-)$‡
1472 } 1465 }	1464	1464	$\delta(CH_2)$‡
1460	1456	1456	$\delta_a(CH_3)$‡
1435	1440 } 1417 }	1440 } 1422 }	$\delta(CH_2)$†‡
1420 } 1400 }		1407	$\nu_s(COO-)$
1380			$\delta_s(CH_3)$
	1297	1297	$tw(CH_2)$
1350–1150			CH_2 wagging progression bands
	1124	1124	$\nu_s(CC)_{all\text{-}trans}$
1100–700			CH_2 rocking progression bands
	1080	1080	$r(CH_2)$‡§
	1063	1063	$\nu(CC)$
920	925	940	$r(CH_3)$†
880	890	890	$\nu(CC)$
720			$r(CH_2)_{all\ in\ phase}$
690			$\delta(COO-)$‡
540			$w(COO-)$‡
	400–90	400–90	LAM†‡§

†Crystalline structure dependent wavenumber.
‡Temperature dependent wavenumber.
§Chain length dependent wavenumber.

different authors and here, except for $Pb(C10)_2$ [8], in which concordance with our values is good. This could be due to the special and complicated behaviour of this series of compounds (samples obtained by crystallization and from the melting process have a completely different behaviour), and to the influence of impurities on the temperatures and enthalpies of the transitions. When the sample is not sufficiently pure, pretransitional effects (appearing as small or large shoulders) modify considerably the base line of the thermograms, and, consequently, affect not only the temperature, but also the enthalpy of the transitions.

A peculiar behaviour is found in $Pb(C7)_2$: it is the only member of the series with two solid–solid transitions, the second one very near to and overlapped with the fusion transition. The same was observed by Adeosun and Sime [5], as indicated in a table footnote in their article.

In figure 7, temperatures of transition versus n are shown. The liquid crystal (LC) phase is present only in the

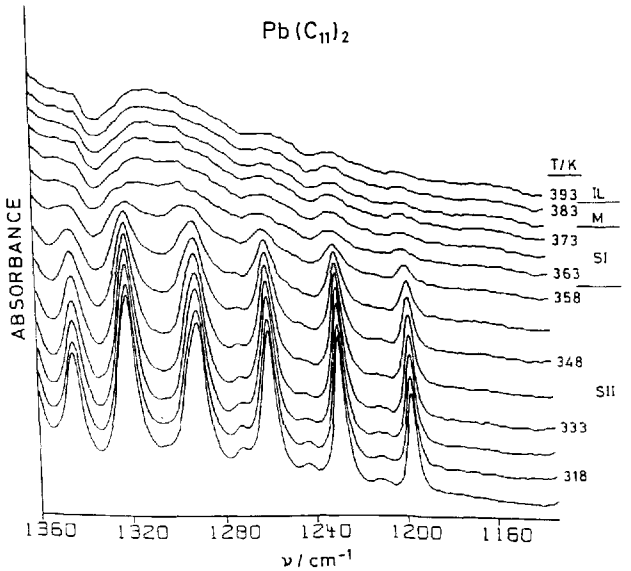

Figure 5. Infrared spectra of $Pb(C11)_2$ (1400–1100 cm^{-1}) at different temperatures. Each sprectum has been shifted vertically without any change of scale (IL, isotropic liquid; M, mesophase; SI and SII, solid phases).

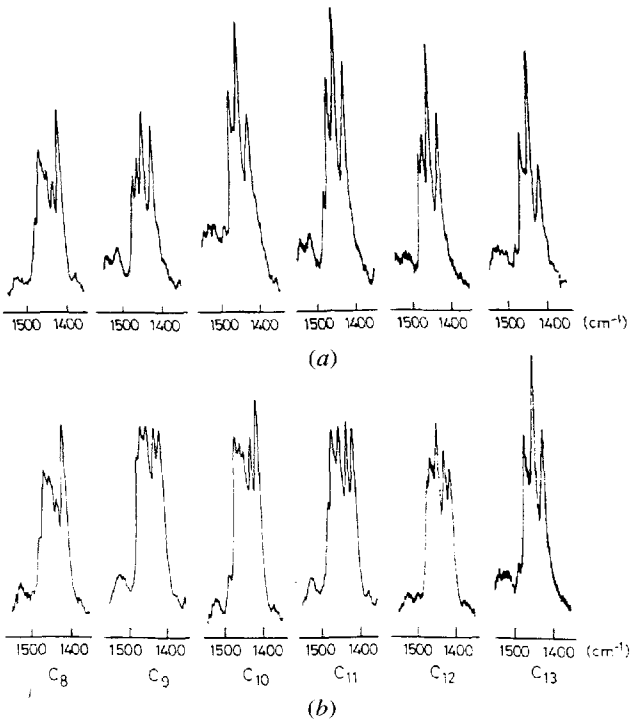

Figure 6. Raman spectra of $Pb(Cn)_2$ ($n = 8$–10) in the range 1500–1400 cm^{-1}; (*a*) recrystallized samples; (*b*) premelted samples.

lower members of the series for $6 \leq n \leq 12$. The temperatures of solid–solid and fusion transitions increase with increase in the number of carbons, as expected. The temperature of the liquid crystal to isotropic liquid

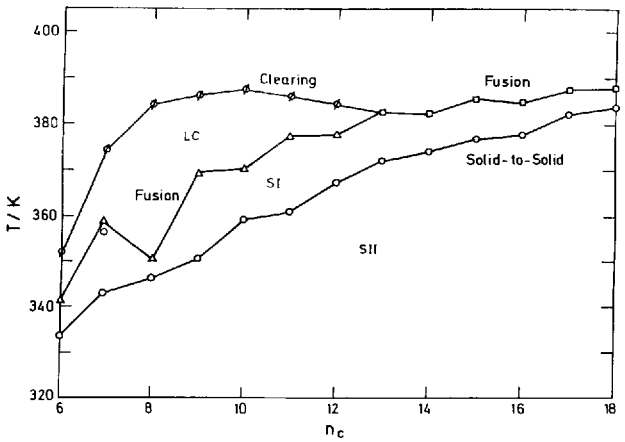

Figure 7. Transition temperatures versus n for the Pb(Cn)$_2$ series.

transition ('clearing') increases very rapidly for the lower members, reaching a maximum at $n = 10$.

4.2. *Odd–even effects*

An odd–even effect in the SII–SI transition temperature is observed. This effect could be due, according to the Malkin rule [21], to a tilted alignment of the chains with respect to the lamellar planes in the SII phase, producing a different packing of the lamellae with respect to the end-to-end coupling of their CH_3 groups, depending on the odd or even number of carbons. If the chains were perpendicular to the lamellae, this effect would be completely ruled out. The Malkin effect observed supports the assignment of the mesophase as smectic C.

For the SI–LC transition (fusion), a more pronounced odd–even effect is observed. Since IR results show that in the SI phase the predominant all-*trans*-conformation of the alkyl chains has already been lost, this alternation cannot be explained by a Malkin effect. Therefore, this behaviour could be due to an odd–even effect similar to that described for the first time by Marcelja [22] for nematic to isotropic transitions. This effect is related to the parallel packing of the chains.

In the case of Pb(C8)$_2$, DSC (see pretransitional shoulder in figure 1) and FTIR (see figure 8) results show that the fusion of the chains starts at lower temperatures than for other members of the series, pointing to a more disordered SI phase. This could be the explanation for the lower than expected fusion temperature observed for this compound (see figure 7).

The two odd–even effects are also seen in both ΔH and ΔS versus T plots (see figure 9), confirming that the molecular axis is not perpendicular to the crystal planes (SII–SI transition), and that the fusion takes place with separation of the parallel chains. This fusion would also involve the ionic fusion of the layers. It is clear that the size of the chains has a big influence on both the solid–solid and fusion transitions, as ΔH increases for both transitions with n. The internal rotation of the CH_2 groups and van der Waals interactions between chains would contribute to the enthalpies of both transitions. The enthalpy of the 'clearing' transition in the lead(II) series is very low and decreases until $n = 12$, which is the last member with a liquid crystal phase.

4.3. *CH_2 contribution to the thermal functions*

From the representation of the total ΔH and ΔS of transition versus the number of carbons, the value of the slope was determined by least squares adjustment of all the data. Since there are two chains per molecule, these values should correspond to twice the value of the contribution per CH_2 group to the corresponding thermal property. No differences for the values of the slopes were found whether the odd or even members were adjusted. The results were: $\Delta H = 4820 \pm 1\,\mathrm{J\,mol^{-1}}$ of CH_2 groups and $\Delta S = 12{\cdot}15 \pm 0{\cdot}05\,\mathrm{J\,K^{-1}}$ per mol of CH_2 groups. Nagle and Goldstein [23] determined the contribution per CH_2 group to the enthalpy and entropy of fusion of polyethylene as $4100\,\mathrm{J\,mol^{-1}}$ and $9{\cdot}87\,\mathrm{J\,K^{-1}\,mol^{-1}}$, respectively. According to these authors these values involve a conformational contribution term, a cohesive van der Waals energy term and a volume terms (only in the case of entropy). Although the ΔH value found for the

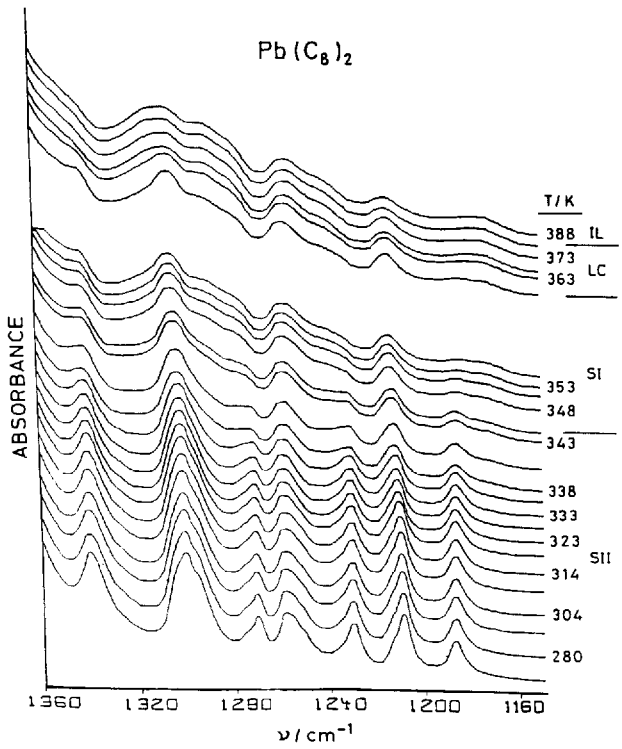

Figure 8. Infrared spectrum of Pb(C8)$_2$ in the 1400–1100 cm^{-1} range. Spectra displaced as in figure 5.

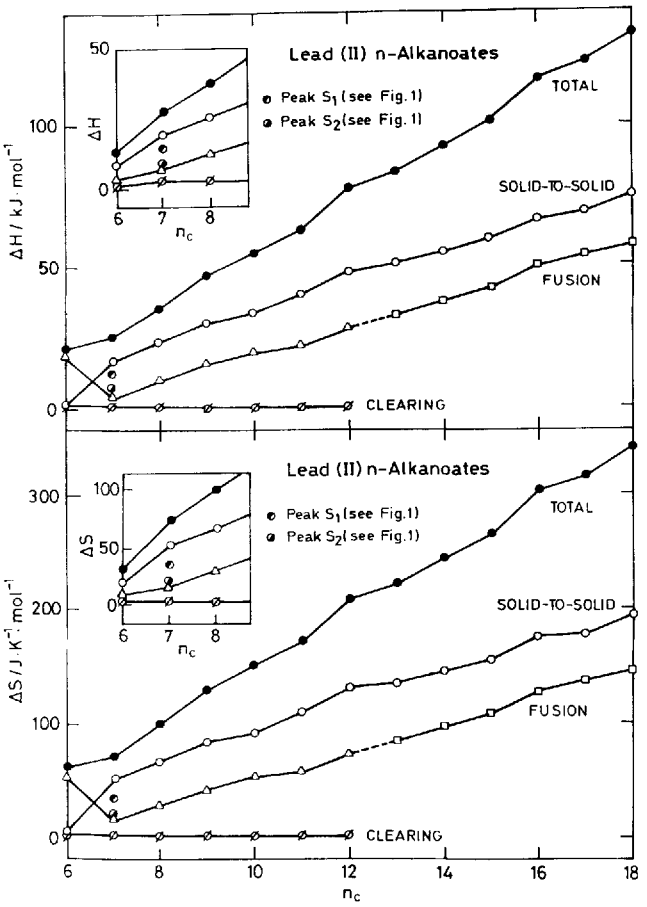

Figure 9. ΔH and ΔS versus n, for the Pb(Cn)$_2$ series. (Ordinate 'zero' displaced for clearness).

lead(II) alkanoates is close to that found for polyethylene, that of ΔS is higher, pointing to a higher contribution of the volume term in this soap series.

In figure 9, the two different behaviours of Pb(C6)$_2$ (see figure 1) are represented. The one corresponding to the metastable state follows the general tendency of the higher members of the series (insets of figure 9), but the enthalpies corresponding to the phase transitions registered after achieving thermal equilibrium are different, the enthalpy of the fusion process being higher than for the solid–solid change, in contrast with the general behaviour of the other members of the series. The strong ionic interaction between the layers, which are closer to each other in the lower members of the series, could be the origin of this double behaviour.

4.4. *Molar heat capacities*

In figure 10, the curves for the molar heat capacities for the low temperature solid phases versus n (see table 2) are shown for all the compounds studied. In some of them, the heat capacity increases very rapidly at the higher temperature end, as a pretransitional effect of the solid–solid phase transition. At low temperatures, the different lattice heat capacity curves are parallel to each other, in agreement with the fact that no solid–solid transition was observed down to liquid nitrogen temperature, pointing to an iso-crystalline structure for all of them. Adeosun and Sime [4, 5] measured the heat capacity for the three phases of this series of compounds. Although for the solid phases, they give only data in a graphic form, the agreement with our values seems to be within experimental error, except for the heat capacities of Pb(C9)$_2$ and Pb(C11)$_2$ at around 325 K, where they find an intersection on the heat capacity versus T curves.

4.5. *Vibrational spectroscopy and the condis phase*

As pointed out above, Raman spectra (and to a lesser extent infrared spectra too) of lead carboxylates Pb(Cn)$_2$ with $n = 9$–12 depend on the thermal history of the sample. This is due to the polytipism present in this kind of compound. Raman results indicate (see figure 6) that this polytipism is a consequence of changes in the packing of the alkyl chains. For soaps with $n > 13$ and $n < 8$, no differences between the Raman spectra of the recrystallized and premelted samples are obtained.

The structural modifications taking place in the samples when the temperature increases and in the different phases have been followed by recording the infrared spectra every 5 K. These infrared data show (see figure 5) that conformational disorder is higher in solid **I** where the all-*trans*-conformation of the alkyl chain is lost. This

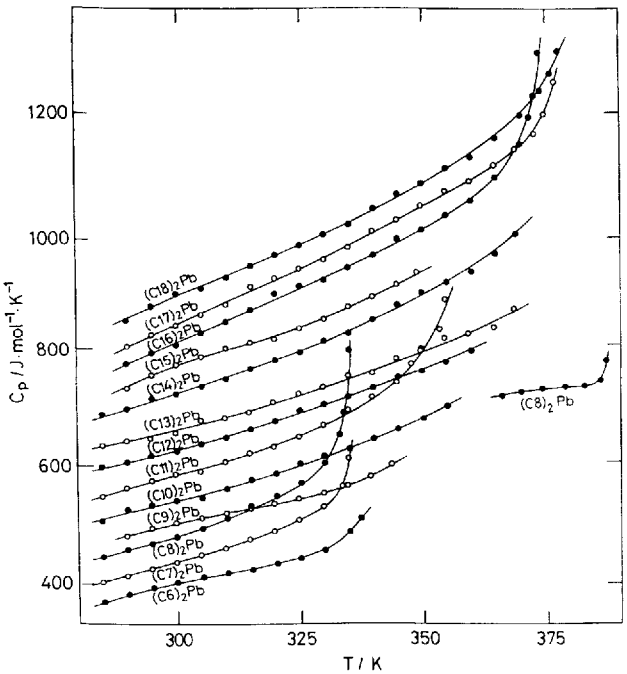

Figure 10. Molar heat capacities versus temperature, for the Pb(Cn)$_2$ series.

behaviour is observed both in crystallized and premelted samples. Therefore, solid **I** is a conformationally disordered phase. However, since polarizing light microscopy observations suggest that the sample still remains as a solid phase, this intermediate phase seems to be a conformationally disordered crystal like those described by Wunderlich [24].

This result agrees with previous studies on the temperature dependence of the Raman and NMR spectra of some members of this series [10, 11] that showed conformational disorder of the intermediate phase. In addition, the dependence of ΔH and ΔS on the number of carbon atoms in the alkyl chain (see figure 9) corroborates the importance of conformational disorder at this phase transition [24].

References

[1] FRANZOSINI, P., and SANESI, M., 1980, *Thermodynamic and Transport Properties of Organic Salts* (Pergamon Press).

[2] MIRNAYA, T. M., PRISYAZHNYI, V. D., and SHCHERBAKOV, V. A., 1989, *Russ. Chem. Rev,* **58,** 821.

[3] GARCIA, M. V., REDONDO, M. I., CHEDA, J. A. R., WESTRUM, JR, E. F., and FERNANDEZ-MARTIN, F., 1994, *Appl. Spectrosc.*, **48,** 338.

[4] ADEOSUN, S. O., and SIME, S. J., 1976, *Thermochim. Acta*, **17,** 351.

[5] ADEOSUN, S. O., and SIME, S. J., 1978, *Thermochim. Acta*, **27,** 319.

[6] ELLIS, H. A., 1986, *Molec. Crystals liq. Crystals*, **139,** 281.

[7] ELLIS, H. A., and DE VRIES, A., 1988, *Molec. Crystals liq. Crystals*, **163,** 133.

[8] AMORIN DA COSTA, A. M., BURROWS, H. D., GERALDES, C. F. G. C., TEIXEIRA-DIAS, J. J. C., BAZUIN, C. G., GUILLON, D., SKOULIOS, A., BLACKMORE, E., TIDDY, G. J. T., and TURNER, D. L., 1986, *Liq. Crystals*, **1,** 215.

[9] BURROWS, H. D., GERALDES, C. F. G. C., PINHEIRO, R. K., HARRIS, R. K., and SEBALD, A., 1988, *Liq. Crystals*, **3,** 853.

[10] BAZUIN, C. G., GUILLON, D., SKOULIOS, A., AMORINDA COSTA, A. M., BURROWS, H. D., GERALDES, C. F. G. C., TEIXEIRA-DIAS, J. J. C., BLACKMORE, E., and TIDDY, G. J. T., 1988, *Liq. Crystals*, **3,** 1655.

[11] FEIO, G., BURROWS, H. D., GERALDES, C. F. G., and PINHEIRO, T. J. T., 1991, *Liq. Crystals*, **9,** 417.

[12] BURROWS, H. D., 1990, *The Structure, Dynamics, and Equilibrium of Colloidal Systems*, edited by D. M. Bloor and E. Wyn-Jones (Kluwer Academic Publishers), pp. 415–476.

[13] FEIO, G., BURROWS, H. D., GERALDES, C. F. G. C., and PINHEIRO, T. J. T., 1993, *J. chem. Soc. Faraday Trans.*, **89,** 3117.

[14] AKANNI, M. S., OKOH, E. K., BURROWS, H. D., and ELLIS, H. A., 1992, *Thermochim. Acta*, **208,** 1.

[15] BURROWS, H. D., GERALDES, C. F. G. C., MIGUEL, M. G. M., PINHEIRO, T. J. T., CRUZ PINTO, J. J. C., 1992, *Thermochim. Acta*, **206,** 203.

[16] EKWUNIFE, M. E., NWACHUKWU, M. U., RINEHART, F. P., and SIME, S. J., 1975, *J. chem. Soc. Faraday Trans. I*, **75,** 532.

[17] MARTI, E. E., 1973, *Thermochim. Acta*, **5,** 173.

[18] SATO, K., and KOBAYASHI, M., 1991, *Crystals, Growth, Properties and Appplications: Organic Crystals*, Vol. 1, edited by N. Kare (Springer-Verlag), p. 65.

[19] GRAY, G. W., and GOODBY, J. W., 1984, *Smectic Liquid Crystals: Textures and Structures* (Leonard Hill).

[20] CHAPMAN, D., 1962, *Chem. Rev.* **62,** 433.

[21] MALKIN, T., 1952, *Progress in the Chemistry of Fats and Other Lipids*, edited by T. L. Hollmann (Pergamon Press), Chap. 1.

[22] MARCELJA, S., 1974, *J. chem. Phys.*, **60,** 3599.

[23] NAGLE, J. F., and GOLDSTEIN, M., 1985, *Macromolecules*, **18,** 2643.

[24] WUNDERLICH, B., MOLLER, M., GREBOWICK, J., and BAUR, H., 1988, *Conformational Motion and Disorder in Low and High Molecular Mass Crystals*, edited by H. Höcker (Springer-Verlag), Chap. 1.